Environmental Science Advances

ROYAL SOCIETY OF CHEMISTRY

PAPER

View Article Online
View Journal | View Issue

Check for updates

Cite this: *Environ. Sci.: Adv.*, 2023, **2**, 462

Planetary ball milling induced piezocatalysis for dye degradation using $BaTiO_3$ ceramics

Akshay Gaur, Vishal Singh Chauhan* and Rahul Vaish *

Received 30th August 2022
Accepted 23rd January 2023

DOI: 10.1039/d2va00210h

rsc.li/esadvances

Piezocatalysis is one of the emerging areas utilized in environmental remediation. The process generally makes use of an ultrasonicator for separating the charges. However, piezocatalysis through an ultrasonicator is just limited to laboratory-scale remediation, and there are various other limitations associated with its usage. Ball milling (BM) is normally utilized for mixing, grinding, and synthesis of precursors. However, BM in the present study is utilized as a piezocatalysis system where a rotating planetary disk and collisions of milling balls generate enough force that abundant reactive species, responsible for the degradation of organic dyes, are produced. For this, methylene blue (MB) dye was used as a pollutant in water with ~5 mg L^{-1} concentration and $BaTiO_3$ powder as a piezocatalyst. At 200 rpm, the MB dye degradation was ~36, ~61, and ~54%, respectively, with 5, 10, and 15 Zr balls using 0.15 g of $BaTiO_3$ ceramic powder. The potential of BM as a piezocatalysis system was further analyzed using various parameters (*e.g.*, speed of BM and the number of milling balls), volume of MB dye, and dose of $BaTiO_3$ ceramic powder.

Environmental significance

Rapid globalisation has resulted in environmental contamination and consequently deterioration of water quality can be witnessed due to the accumulation of toxic compounds. Piezocatalysis is one of the emerging processes utilized in water cleaning applications. When a mechanical force is subjected to piezocatalyst, reactive oxygen species (ROS) are produced, responsible for weakening organic pollutants in water. At present, the pressure generated by ultrasonication's pulsed acoustic cavitation in solution induces an alternative polarisation potential in piezocatalysts. However, ultrasonication is limited by the use of acoustic cavitation, which restrained the potential industrial application of piezocatalysts. Thus, utilizing ball milling as a source excitor for degrading organic pollutants is a green and facile approach. Effective degradation of methylene blue dye (30 and 50 mL) supports such statements.

1. Introduction

Rapid globalization has resulted in environmental contamination and deteriorated the quality of soil, water, and air due to the accumulation of toxic compounds.[1] All constituents of an ecosystem are vulnerable to the pernicious effects of these chemicals. Water, in particular, is one of the most vital elements of the ecosystem and deserves special care. To solve contaminated water-related issues, various processes are utilized in water treatment.[2] Piezocatalysis is one such process that uses a direct piezoelectric effect by converting mechanical energy into electrochemical energy. The advantage of piezocatalysis process is that it is independent of electricity and light source and relies on mechanical energy.[3] The piezocatalysis process resembles processes such as electrocatalysis and photocatalysis; however, in the case of the piezocatalysis process, the energy source needed would be a mechanical force.[4–6] The mechanical energy for the piezocatalysis process can also be in the form of natural sources such as wind and waves. When a mechanical source is subjected to a piezocatalyst, a potential difference on the surfaces is formed due to strong driving electric potential difference created due to the separation of electrons and holes.[7,8] This separation of charges, *i.e.*, electrons and holes, is responsible for azo dye decolorization in aqueous solution.[9] An electron and a hole can take part in a redox reaction because of the potential difference created on the surface of the piezocatalyst by an external force (mechanical energy). When an electron reacts with dissolved oxygen in water, it creates superoxide radicals, while holes create hydroxyl radicals.[10] Ferroelectric materials are the subclass of piezoelectric materials having a unique characteristic of retaining electric potential at a different location on its surfaces.[11] $BaTiO_3$ is one of the classical ferroelectric materials widely studied due to its high dielectric properties, ferroelectricity, optical, piezoelectric, and other properties.[12] Also, it has a unique property of being crystallized in rhombohedral, orthorhombic, and tetragonal crystal structures based on the crystallization temperature.[13,14] The utilization of $BaTiO_3$ as piezocatalyst with certain modifications is well reported in the literature for organic dye removal through piezocatalysis process.[15–19] However, the screening

School of Mechanical and Materials Engineering, Indian Institute of Technology Mandi, Mandi, Himachal Pradesh 175005, India. E-mail: vsc@iitmandi.ac.in; rahul@iitmandi.ac.in

Open Access Article. Published on 23 ianuarie 2023. Downloaded on 07.01.2026 20:12:19.
This article is licensed under a Creative Commons Attribution-NonCommercial 3.0 Unported Licence.

© 2023 The Author(s). Published by the Royal Society of Chemistry

Open Access Article. Published on 23 ianuarie 2023. Downloaded on 07.01.2026 20:12:19.
This article is licensed under a Creative Commons Attribution-NonCommercial 3.0 Unported Licence.

effect in free charges restricts the piezocatalysis process, resulting in decreased efficiency. To overcome this problem, the synthesis of piezocatalyst is done by considering parameters such as morphology and particle size or by creating a heterojunction between semiconductors for degrading organic dyes.[20–23] Doping of elements such as calcium (Ca), zirconium (Zr), strontium (Sr), and samarium (Sm) in $BaTiO_3$ ceramics have shown enhanced piezocatalytic activities in environmental remediation.[24–29] By modifying numerous parameters in the synthesis route of piezocatalyst, the efficiency of degrading organic dyes *via* piezocatalysis is significantly enhanced. But the efficiency with which organic dyes should be degraded by the piezocatalysis process is still unsatisfactory, and large-scale piezocatalytic systems have not been explored much. Generally, piezocatalysis process is performed under ultrasonication for polarization modulation in ferroelectric materials.[30] However, limited processing scale and cavitation occurrence due to vibrations produced by ultrasonication still raise question while performing piezocatalysis processes for the treatment of water.[31] Therefore, it becomes necessary to find an effective way of utilizing the piezocatalysis process on a facile and large scale. Ball milling is a simple technique generally used for grinding precursors into fine powder. Apart from the grinding of precursors, the synthesis of oxides or nanocomposites and optimization of structure/phase composition *via* material reactivity and uniformity among elements can be achieved through the ball milling technique.[32–34] Also, with the effect of charge transfer through piezoelectric material in ball milling synthesis of organic molecules, generation of radicals and radical cyclization is possible.[35–37] Ball milling is based on the principle of attrition and impact, where the balls impact each other within a shell/jar resulting in the mixing and grinding of precursors. In recent times, ball milling has been viewed as an external force generator where it can be utilized as a source for environmental remediation.[38,39] Using the ball milling technique, free charges can be effectively separated out, thus building an alternating electric field. To date, the ball milling technique has generally been utilised for grinding precursors and synthesis of materials. However, utilizing it as a source excitor in piezocatalysis process will allow researchers to explore a green and facile method at a larger level. Thus, the present study brings outs a novel prospective of utilizing ball milling technique as a source excitor for degrading MB dye under piezocatalysis process using $BaTiO_3$ (ferroelectric material) as a piezocatalyst.

2. Experimental section

2.1 Synthesis of $BaTiO_3$ powder

$BaTiO_3$ powder was synthesized through a simple solid oxide route reaction method. In a typical method, precursors (~99% pure), barium carbonate ($BaCO_3$) and titanium dioxide (TiO_2), were weighed according to their stoichiometric ratios. Consequently, the weighted mixture was subjected to manual mixing through mortar and pestle for 1 h in a medium of acetone to obtain homogeneity. Thereafter, the reaction mixture was subjected to calcination heat treatment at 1200 °C for 6 h in an electric furnace (Nobertherm).

2.2 Characterization of $BaTiO_3$ sample

Powder X-ray diffraction was employed for determining the phase formation and purity of the synthesized $BaTiO_3$ on an X-ray diffractometer (Rigaku Corporation) with a 9 kW rotating anode having a Cu-Kα source ($\lambda = 1.54$ Å). The obtained X-ray patterns were studied in a range of 20–75° (2θ degree) at a constant scanning rate of $0.03°s^{-1}$. Furthermore, vibration modes within the $BaTiO_3$ powder sample were studied through Raman spectroscopy (HORIBA, Model-Lab RAM HR Evolution, Japan) using a green laser having a 532 nm wavelength. A field emission scanning electron microscope (FE-SEM) was used to assess the surface morphology and size of the synthesized $BaTiO_3$ powder sample. For elemental determination, the X-ray photoelectron spectroscopy (XPS) technique was employed through an X-ray photoelectron spectrophotometer (NEXSA). Further, a UV-visible spectrophotometer (SHIMADZU-2600) was utilized for determining the energy band gap of $BaTiO_3$ powder, calculated through Tauc's plot obtained from diffuse reflectance spectrum (DRS).

2.3 Performance assessment of the piezocatalysis process

Methylene blue (MB) dye with ~5 mg L^{-1} concentration was used as a symbolic organic pollutant in water. Planetary ball mill PM 100 (Retsch) at 100, 200, and 300 rpm was employed as a mechanical energy source. For piezocatalysis assessment, a Teflon-lined milling jar (nominal volume of 125 mL) with a zirconium ball having a 10 mm diameter size (5, 10, and 15 in quantity) was used. For facilitating adsorption–desorption equilibrium, the $BaTiO_3$ sample with varying concentrations (0.15, 0.20, and 0.30 g) was immersed in MB dye (30 and 50 mL in quantity) overnight, powered by a magnetic stirrer. The weakening of the chosen dye concentration using the ball milling technique as a mechanical source and $BaTiO_3$ as a piezocatalyst was estimated by calculating the difference between the initial and final concentration of MB dye. For this, after every 15 min, the tested sample was centrifuged in a 1.5 mL Eppendorf tube, and its absorbance was checked with a UV-visible spectrophotometer (SHIMADZU-2600) in a range of 400–800 nm wavelength.

3. Results and discussions

Fig. 1 depicts the XRD pattern obtained in a 2θ range of 20–75°. The peaks were well matched with JCPDS file no: 05-0626. The absence of any additional peaks confirms the formation of synthesized $BaTiO_3$ ceramic powder. Further splitting of the peak at ~45° (2θ degree) corroborates that the synthesized $BaTiO_3$ ceramic powder crystallized into a single perovskite structure having a tetragonal phase. The peaks in diffraction pattern originating at 22.32°, 31.59°, 38.97°, 44.92°/45.32°, 51.09°, 56.34°, 66.04°, and 70.31° corresponded to Braggs reflection at planes (100), (110), (111), (002)/(200), (201), (202), and (301), respectively. Furthermore, to validate the XRD

Open Access Article. Published on 23 ianuarie 2023. Downloaded on 07.01.2026 20:12:19.
This article is licensed under a Creative Commons Attribution-NonCommercial 3.0 Unported Licence.

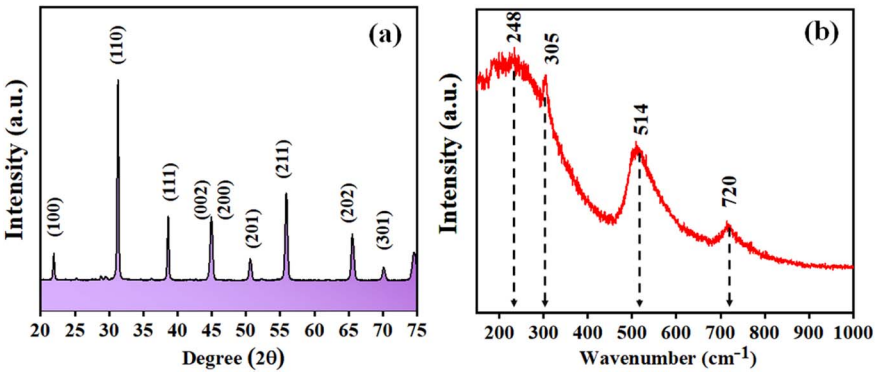

Fig. 1 Synthesized $BaTiO_3$ (a) XRD pattern, (b) Raman spectrum.

pattern, the Raman spectrum of $BaTiO_3$ was done in a range of wavenumber 150–1000 cm^{-1}, as shown in Fig. 1(b). Dominating peaks were observed at 248, 305, 514, and 720 cm^{-1} wavenumbers. Raman spectrum at ~250 and ~515 cm^{-1} corresponds to both phases of $BaTiO_3$, *i.e.*, cubic and tetragonal structure.[40] Nevertheless, the intensity at ~307 and ~715 cm^{-1} wavenumber is specifically due to the tetragonal phase present in $BaTiO_3$.[41] Raman spectrum of the $BaTiO_3$ tetragonal phase comprises four intense bands at positions ~250 (A1 (TO)), ~307 (B1, E (TO + LO)), ~515 (A1(TO), E (TO)) and 715 cm^{-1} (A1(LO), E(LO)).[42,43] The ~307 cm^{-1} wavenumber is the B1 mode, which is due to the absence of symmetry in the TiO_6 (octahedral) structure, whereas A1 symmetry is designated to ~715 cm^{-1} wavenumber, the highest wavenumber longitudinal optical mode.[41]

Fig. 2(a) and (b) display SEM micrographs analyzing the morphology of the synthesized $BaTiO_3$ powder at a certain magnification in 5 and 1 μm scales. It can be seen that there is no specific morphology having an irregular shape with smooth edges. However, at a 1 μm scale, some facets can be observed. The particle size (length in μm) was estimated through ImageJ software and was found to be ~0.500 μm. Furthermore, to collect additional information about the synthesized $BaTiO_3$ powder, the energy band gap through DRS, as shown in Fig. 3(a), was calculated by Tauc's plot displayed in Fig. 3(b). The energy band gap was found to be ~3.19 eV, which matched with the previously reported work in the literature.[44]

Fig. 4(a) displays the XPS survey of $BaTiO_3$ powder in a range of 0–1250 binding energy (eV). The photoelectron peaks at ~285.84, ~458.28 eV, ~529.85 eV, and ~779.20 eV corresponded to C 1s, Ti 2p, O 1s, and Ba3d5 levels. Further, the O1s photoelectron peak was deconvoluted into other peaks at ~528.9, ~530.8, and ~531.95 eV binding energy. The lower BE peak (~528.9 eV) attributes to O^{2-} ions, the middle BE peak (~530.8 eV) to O^{1-} ions, and the upper BE peak (~531.95 eV) to O^{Chem}, or chemically adsorbed oxygen at the surface.[45]

It is very critical to attain adsorption–desorption equilibrium before the piezocatalysis process to differentiate it from degradation achieved through the adsorption process. Once the equilibrium was achieved, the samples were subjected to mechanical force *via* the ball milling technique. There are certainly many factors that need to be thoroughly studied while probing the assessment of the piezocatalysis process through the ball milling technique. These factors are the volume of dye (in mL), the dose of piezocatalyst (grams), the number of balls, and the ball milling speed (in rpm). Initially, 0.15 g of piezocatalyst ($BaTiO_3$) dose was taken for probing 30 mL of ~5 mg L^{-1} concentrated MB dye using 5 balls with ball milling at 100, 200, and 300 rpm. Subsequently, the assessment of piezocatalysis performance through the ball milling technique was further analyzed with 10 and 15 Zr balls at 100, 200, and 300 rpm. Fig. 5(a) shows the absorbance spectrum of ~5 mg L^{-1} concentrated MB dye (30 mL quantity) using 0.15 g of $BaTiO_3$ powder with 10 Zr balls at 200 rpm speed. Additionally, control

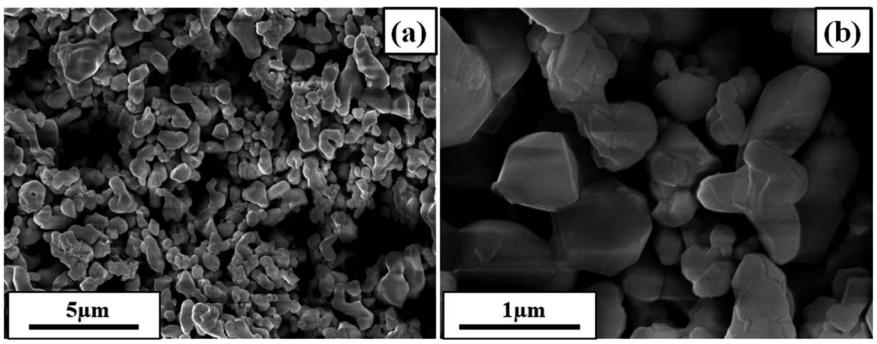

Fig. 2 SEM images of synthesized $BaTiO_3$ at a resolution scale of (a) 5 μm, (b) 1 μm.

 © 2023 The Author(s). Published by the Royal Society of Chemistry

Open Access Article. Published on 23 januarie 2023. Downloaded on 07.01.2026 20:12:19.
This article is licensed under a Creative Commons Attribution-NonCommercial 3.0 Unported Licence.

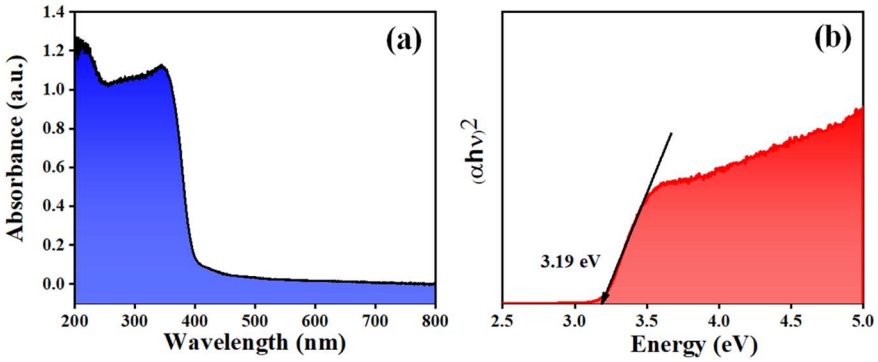

Fig. 3 (a) DRS of $BaTiO_3$, (b) Tauc's plot for energy band gap.

testing of MB dye (without using any piezocatalyst dose) was done in the same jar with the same parameters, *i.e.*, with 10 Zr balls at 200 rpm, and its absorbance spectrum is displayed in Fig. 5(b). The quantification measure of MB dye degradation (d%) is expressed in eqn (1).

$$d\% = \left\{1 - \left(\frac{C}{C_0}\right)\right\} * 100 \quad (1)$$

where"C" and "C_0" represent the final (after every 15 min) and initial concentration of MB dye (~664 nm wavelength in absorbance spectra of MB dye).

On observing the absorbance spectra of MB dye (with 0.15 g of $BaTiO_3$ powder with 10 Zr balls running at 200 rpm speed), the reaction kinetics obtained for piezocatalysis degradation commanded by Langmuir–Hinshelwood (LH) model is expressed in eqn (2).[46]

$$R = \frac{dC_i}{dT} = kKC_i + \frac{kKC_i}{1} \quad (2)$$

where C_i represents the initial molar concentration of MB dye, k corresponds to the rate constant, and K is the adsorption coefficient (on piezocatalyst of MB dye). However, when C_i is less than 10^{-3} M and $kKC_i << 1$, then eqn (2) can be expressed in the form of a first-order kinetic reaction manifested in eqn (3).

$$R = \frac{dC_i}{dT} = kKC_i \quad (3)$$

Further, upon integrating and rearranging eqn (3), a first-order kinetic reaction can be simplified into eqn (4).

$$\ln\frac{C}{C_0} = k_f T \quad (4)$$

In eqn (4), C_0 and C are the initial and final concentrations, and $k_f = kK$ represents a reaction constant. Fig. 5(c)–(e) shows the slope of curve plotted between $\ln\frac{C}{C_0}$ with time (T) in min indicating the pseudo-first order reaction rate.

The obtained values of reaction rate or kinetic rate (k_f) in min^{-1} for a weakening of 30 mL ~5 mg L^{-1} concentrated MB dye by 0.15 g of $BaTiO_3$ powder (piezocatalyst) using 5, 10, and 15 balls at 100, 200, and 300 rpm, respectively, are presented in Fig. 6. It can be seen at the macro-level that there is certainly an enhancement of degradation efficiency with both increases in the number of balls as well as with piezocatalyst dose. For 30 mL of ~5 mg L^{-1} concentrated MB dye using 0.15 g of $BaTiO_3$ powder at 100 rpm speed, the degradation was found to be ~28, ~37, and ~39% using 5, 10, and 15 Zr balls, respectively. At 200 rpm, the degradation was ~36, ~61, and ~54% with 5, 10, and 15 Zr balls, respectively. Furthermore, at 300 rpm, the degradation of MB dye was ~48, ~70, and ~75% with 5, 10, and 15 Zr balls.

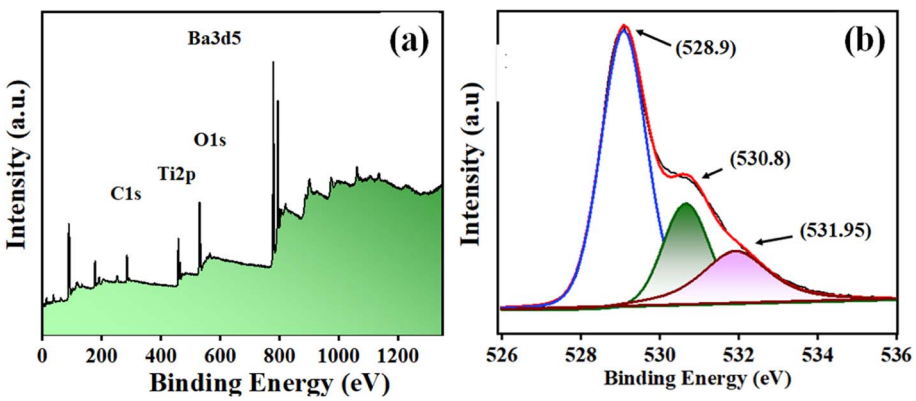

Fig. 4 (a) XPS survey of $BaTiO_3$, (b) deconvoluted survey of O 1s.

Open Access Article. Published on 23 ianuarie 2023. Downloaded on 07.01.2026 20:12:19.
This article is licensed under a Creative Commons Attribution-NonCommercial 3.0 Unported Licence.

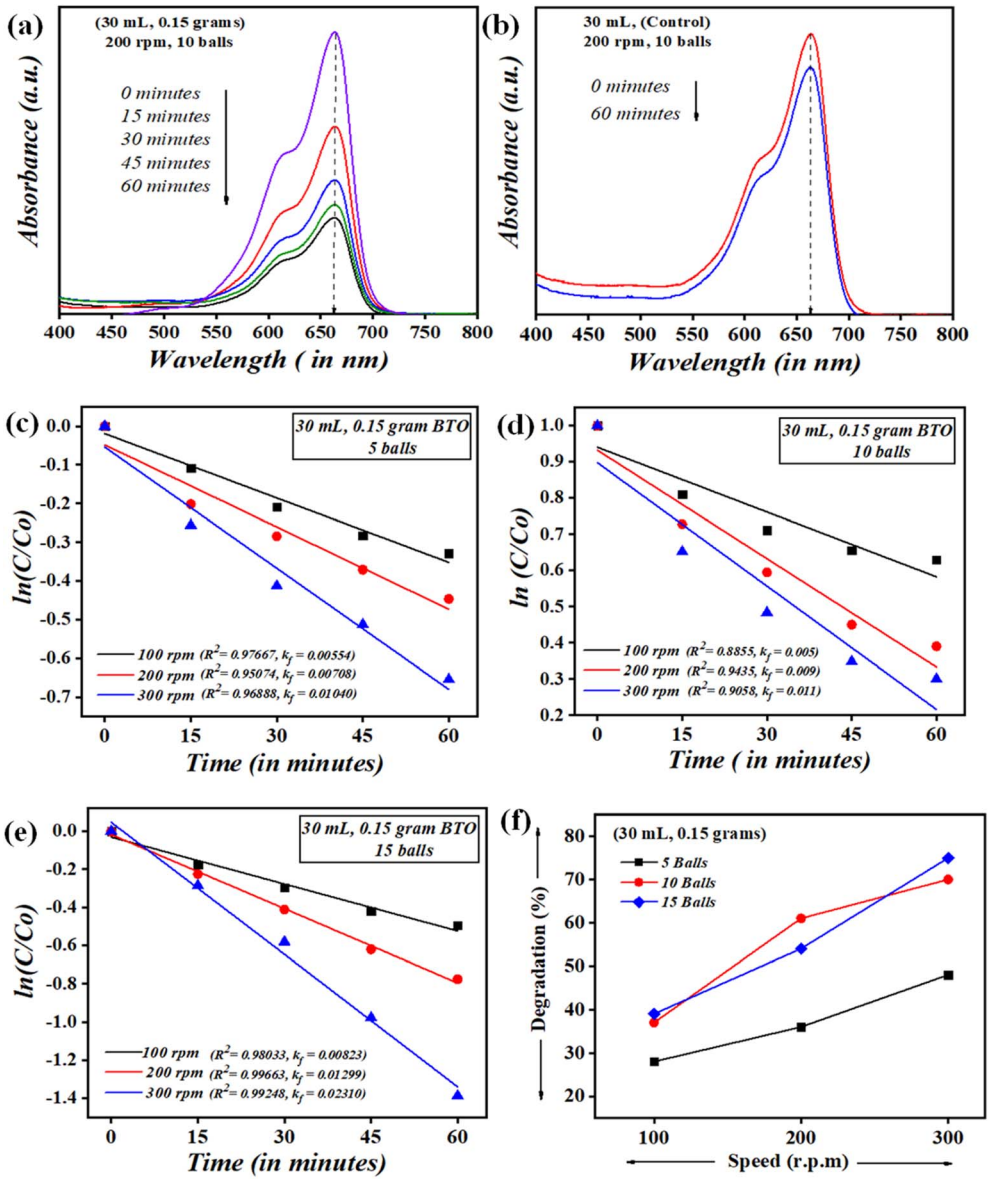

Fig. 5 (a) Absorbance spectra of MB dye using 0.15 g $BaTiO_3$ powder through ball milling at 200 rpm with 10 balls, (b) absorbance spectra of MB dye without using $BaTiO_3$ powder (control) sample through ball milling at 200 rpm with 10 balls, kinetic rate (*kf*) in min^{-1} using 0.15 grams of $BaTiO_3$ powder at 100, 200, and 300 rpm with (c) 5 balls, (d) 10 balls, (e) 15 balls, (f) speed (rpm) *vs.* degradation plot showing % degradation of MB dye using 5, 10, and 15 balls at 100, 200, and 300 rpm speed.

Undoubtedly, with the increase in Zr ball quantity and rpm speed, there is an increment in degradation efficiency. The highest degradation of ~5 mg L^{-1} concentrated MB dye achieved was ~75% with 15 balls at 300 rpm. The speed of ball milling is directly related to the power input needed to run it, and also the number of balls in large quantities can be associated with huge resource availability. ~61% of MB dye degradation gained with 10 balls at 200 rpm using 0.15 g of $BaTiO_3$ powder is comparable if cost and resource availability parameters are taken into consideration. If optimization of Zr ball quantity and rpm speed for the weakening of 30 mL MB dye using 0.15 g of piezocatalyst is quantified, then surely ball milling at 200 rpm with 10 Zr balls can be termed as a king of blind. Thus, 200 rpm and 10 Zr balls were fixed for further piezocatalysis performance assessments through ball milling.

It is rational that with an increase in piezocatalyst ($BaTiO_3$ powder) dose, the efficiency of degradation will increase. For this, piezocatalysis assessment was demonstrated by increasing the piezocatalyst dose to 0.20 and 0.30 g at 200 rpm with 10 Zr balls, and the degradation calculated using eqn (1) was found to be ~66 and ~77%, as shown in Fig. 7(a). Additionally, in the present study, piezocatalysis assessment through ball milling was done by taking 50 mL of MB dye using 0.15, 0.20, and 0.30 g of $BaTiO_3$ powder at 200 rpm with 10 Zr balls. This was done to check the potential of utilizing ball milling at a mass level, as the intention of introducing the ball milling technique for

 © 2023 The Author(s). Published by the Royal Society of Chemistry

Open Access Article. Published on 23 ianuarie 2023. Downloaded on 07.01.2026 20:12:19.
This article is licensed under a Creative Commons Attribution-NonCommercial 3.0 Unported Licence.

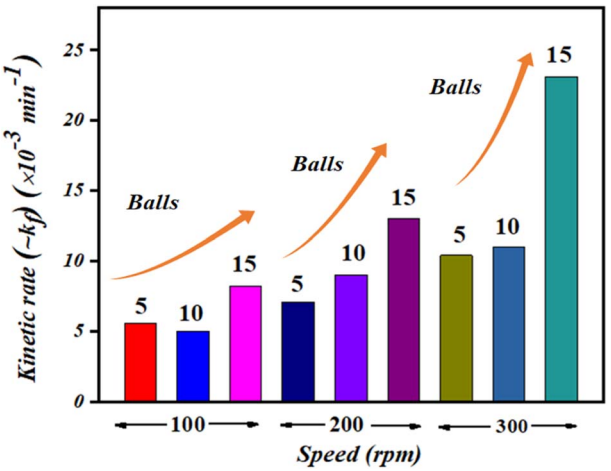

Fig. 6 Kinetic rate (*kf*) in min^{-1} of MB dye degradation using 5, 10, and 15 balls at 100, 200, and 300 rpm.

degrading pollutants present in the water through the piezocatalysis process was to scale it at a mass level. The degradation was found to be ~19, ~35, and ~48% with 0.15, 0.20, and 0.30 g of $BaTiO_3$ powder, respectively, at 200 rpm using 10 balls, as displayed in Fig. 7(b).

The formation and bursting of cavities lead to the degradation of MB dye, and thus at 200 rpm with 10 milling balls, ~18% degradation MB dye (30 mL) is observed. Furthermore, to differentiate other catalytic processes, such as the triboelectric process or for assessing non-piezoelectric control, the degradation of MB dye was observed using 0.3 g of TiO_2 (a non-piezoelectric material) under 200 rpm using 10 balls in 60 min. The degradation of MB dye (30 mL) was found to be ~25% in 60 min and is shown in Fig. 8.

Fig. 8(b) shows a comparison of degradation of MB dye (30 mL having concentration ~5 mg L^{-1}) achieved using 0.3 g of $BaTiO_3$ (piezoelectric material), TiO_2 (non-piezoelectric material), and without using any catalyst dose under 200 rpm using 10 balls in 60 min. The degradation was ~77, ~25 and ~18%, respectively, in 60 min using ball milling. The comparison validates the ignorance of any other process, such as the triboelectric process, and confirms the generation of reactive species through the piezoelectric effect during the collision of balls (piezoelectric material stuck between the balls).

A non-centrosymmetric structure, a prerequisite for piezocatalysis activity in the present study, was fulfilled by a tetragonal phase obtained through $BaTiO_3$ powder. Further, the weakening of MB dye using the ball milling technique through the piezocatalysis process is possible due to the charge separation caused by the impact force generated by milling balls within a jar. The $BaTiO_3$ particles flowing with the dye get stuck between the balls, and the impact force creates charge separation onto the surface of the piezocatalyst. The positive (h^+) and negative charges (e^-) participate in the redox reaction, and reactive species are generated. These reactive species break the heterocyclic structure of MB dye molecules, resulting in the decomposition or weakening of the dye. Fig. 9 shows the ball milling used in the present study and a pictorial representation of the weakening of MB dye through the reduction and oxidation process (REDOX reaction). The degradation of MB dye through the piezocatalysis process can be well understood through the following eqn (5)–(8)

$$BaTiO_3 + \text{Impact force (through balls)} \rightarrow h^+ + e^- \quad (5)$$

$$O_2 \text{ adsorbed} + e^- \rightarrow {}^{\bullet}O_2^- \quad (6)$$

$$OH^- + h^+ \rightarrow {}^{\bullet}OH \quad (7)$$

$$\text{MB dye} + ({}^{\bullet}OH/{}^{\bullet}O_2^-) \rightarrow \text{dye degradation} \quad (8)$$

To analyze the piezocatalysis process using ball milling, the piezocatalysis effect theory can be endorsed, where the induced potential can be viewed as a function of applied force. The relation between strain-induced potential and applied force can be expressed in eqn (9).[47]

$$V = f_n d_{xy} l_x \varepsilon_{rx} \varepsilon_0 \quad (9)$$

where "*V*" is the potential induced on the piezocatalyst surface due to applied force, f_n represents an applied normal force in *y*

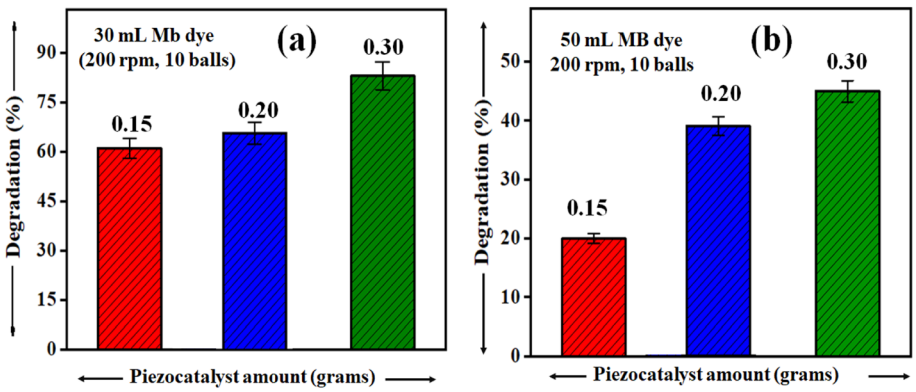

Fig. 7 Degradation of ~ 5 mg L^{-1} concentrated MB dye at 200 rpm milling speed using 0.15, 0.20, and 0.30 grams of $BaTiO_3$ powder for (a) 30 mL and (b) 50 mL.

Open Access Article. Published on 23 ianuarie 2023. Downloaded on 07.01.2026 20:12:19.
This article is licensed under a Creative Commons Attribution-NonCommercial 3.0 Unported Licence.

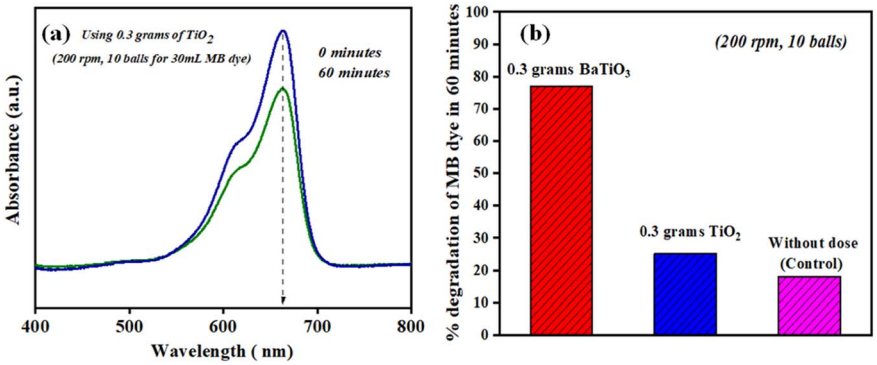

Fig. 8 (a) Absorbance spectra of MB dye using 0.3 g of TiO_2 (non-piezoelectric material) in 60 min with ball milling at 200 rpm using 10 balls, (b) % degradation of MB dye in 60 min using 0.3 g of $BaTiO_3$, TiO_2, and without using any catalyst in 60 min with ball milling at 200 rpm using 10 balls.

coordinate, d_{xy} indicates piezoelectric coefficient, l_x is the length of $BaTiO_3$ in coordinates, ε_{rx} and ε_0 denote the relative permittivity and permittivity of free space. It can be seen in eqn (9) that among all factors, f_n has dominant weightage and can be concluded as a function of induced potential. However, in the ball milling-assisted piezocatalysis process, the applied force on the piezocatalyst has a direct relation with ball milling parameters. A sports model was adopted, expressed in the following eqn (10)–(13).[48,49]

$$f_n = p\pi r^2 \tag{10}$$

$$p = g_p v^{0.4}(\rho/E_e)^{0.2}E_e \tag{11}$$

$$v = \sqrt{(\Omega r_d)^2 + (\Omega - \omega)^2 r_v^2 + 2\Omega(\Omega - \omega) r_d r_v \cos\phi} \tag{12}$$

$$\cos\phi = -\frac{r_v(\Omega - \omega)^2}{r\Omega^2} \tag{13}$$

where p denotes the normal pressure between balls during a collision, g_p is the geometry coefficient, ρ represents the density of balls, v is the normal velocity, and E_e denotes modulus of flexibility. For the sports model, several assumptions are made, and as an outcome of this, in the ball mill mechanism, the trajectory of milling balls can be seen as leaving from position (B1) to position (B2), as shown in Fig. 10(a) ϕ represents the rotation angle of the milling ball, Ω and ω denote the angular velocity of the planetary disk and vial measured at a radius indicated as r and r_d. From the above discussions, it is observed that the weakening of MB dye through the piezocatalysis process using the ball milling technique is directly proportional to the force being applied through milling balls. Furthermore, the applied force can be seen as a function of the velocity of both the planetary disk as well as balls colliding within a jar. Thus, as observed with both increase in speed as well as milling ball quantity, there is an enhancement of MB dye degradation. Fig. 6 validates the statement as for degrading 30 mL ~5 mg L^{-1} concentrated MB dye using 0.15 g of $BaTiO_3$ powder, the approximate kinetic rate ($\sim k_f$) value can be seen increasing from 5.5×10^{-3} to 10×10^{-3} min^{-1}, 5×10^{-3} to 10×10^{-3} min^{-1}, and 8.2×10^{-3} to 23

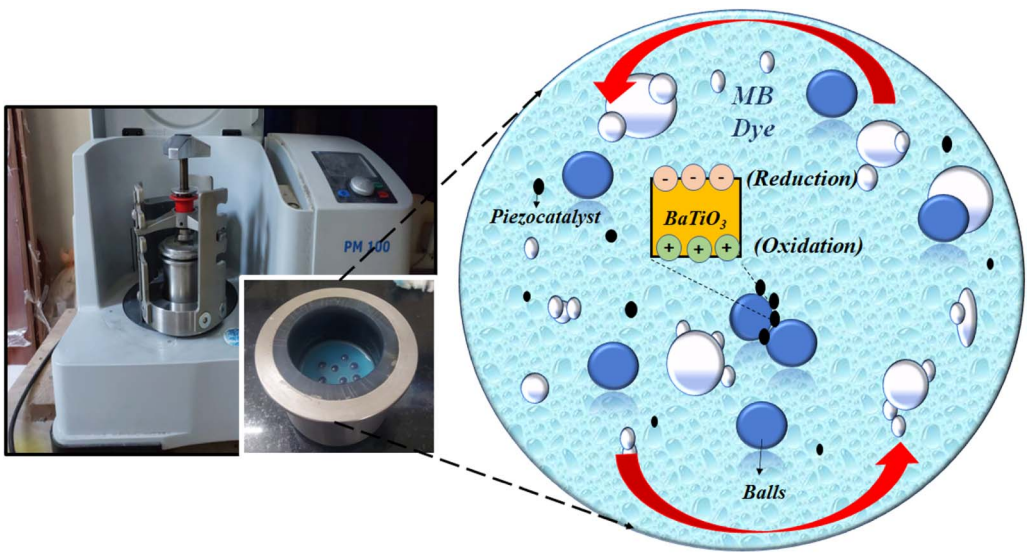

Fig. 9 Schematic representation of piezocatalysis process induced from ball milling for MB dye degradation.

© 2023 The Author(s). Published by the Royal Society of Chemistry

Open Access Article. Published on 23 ianuarie 2023. Downloaded on 07.01.2026 20:12:19.
This article is licensed under a Creative Commons Attribution-NonCommercial 3.0 Unported Licence.

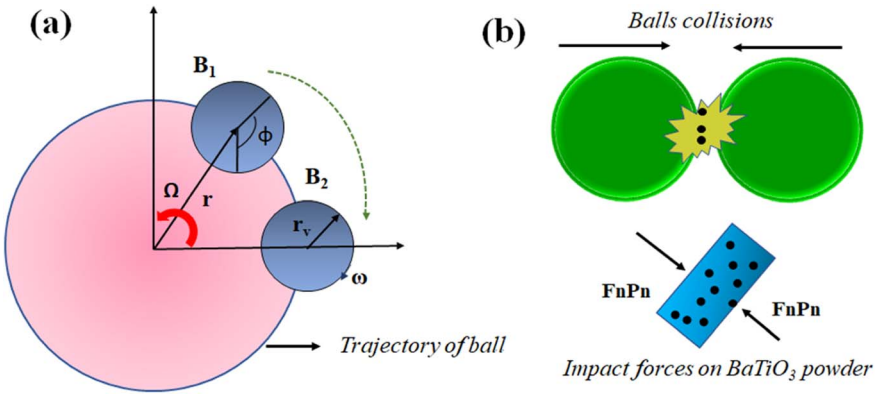

Fig. 10 (a) Trajectory of balls in planetary motion, (b) mechanics of balls for generating piezocatalysis in $BaTiO_3$ powder.

$\times 10^{-3}$ min^{-1} at 5, 10, and 15 milling balls, respectively, with an increase in speed from 100 to 300 rpm. Further, there is an increment in the kinetic rate ($\sim k_f$) from 5.5 $\times$ 10^{-3} to 8.2 $\times$ 10^{-3} min^{-1}, 7 $\times$ 10^{-3} to 13 $\times$ 10^{-3} min^{-1}, and 10 $\times$ 10^{-3} to 23 $\times$ 10^{-3} min^{-1} at 100, 200, and 300 rpm with an increase in ball quantity from 5 to 15.

The milling balls rotate on their axis combined with the rotation generated through the planetary disk in the ball milling machine. Due to this combined motion, the milling ball follows a random path and collides with other milling balls contained within a jar. An increase in speed causes more random motion of milling balls within the jar resulting in more collisions, whereas increasing ball quantity reduces the path distance between the collision of the balls, whereas the combined effect of increasing speed and quantity of milling balls causes more impact force on $BaTiO_3$ powder. In ball milling, the piezocatalyst contained in MB dye following cyclonic motion comes in between the collision of milling balls. Thus, during a collision, an impact force is generated on the $BaTiO_3$ particles due to which induced potential as a result of charge separation is created on the surface of $BaTiO_3$ powder. The schematic presentation of $BaTiO_3$ powder being stuck between the milling balls during collision is shown in Fig. 10(b).

The temperature in the piezocatalysis process plays a significant role as in the case of piezocatalysis process, and the localised temperature reaches up to 4000–5000 K and generates a shock wave up to $\sim 10^8$ Pa pressure when an ultrasonicator is used for generating vibrations.[50] Dye degradation due to the piezocatalysis process sourced by an ultrasonicator has high-frequency vibrations ($\sim$30 kHz), which create cavities in the dye. Due to this increase in temperature and high-pressure waves, an organic dye weakens on its own without any influence of the piezocatalyst. This phenomenon is known as the sonocatalysis or thermolysis process. However, in the case of the ball milling technique, low-frequency vibrations are generated as compared to the ultrasonicator. Although fewer cavities are formed in the ball milling technique as compared to an ultrasonicator in the piezocatalysis process, due to turbulence, the degradation of dye is possible. Furthermore, as discussed, the increased temperature can be a prime factor for the self-degradation of dye. In the present study of piezocatalysis assessment through ball milling, the temperature difference (before and after the piezocatalysis process) measured by thermocouple was found to be negligible, although, from the previous literature, it is observed that a temperature of $\sim$50 °C is attained in ball milling in 1 h of milling.[51] However, in the present study, the noticed MB dye degradation of the controlled sample (without using any $BaTiO_3$ powder) is due to some cavities formed by milling balls following random paths while ball milling was running at a certain speed.

The ball mill technique is employed to grind or mix precursors, which is done by rotating milling balls within a jar filled with precursors in either a liquid medium or dry state. Due to this continued mixing for a long duration in ball milling, there is a reduction in particle size. In fact, in some cases, the precursors are milled for a long duration to reach particles at a nano-scale. In the piezocatalysis process, the surface area of the piezocatalyst plays an important role. As with small-sized particles, the more exposed surface area will be available for piezocatalytic activity to occur. For investigating the change in morphology and size reduction of piezocatalyst ($BaTiO_3$ powder), SEM images before and after the milling operation were compared. The data revealing the information about particle size and morphology before and after milling is shown in Fig. 11(a) and (b).

It was found that after 60 min of ball milling at 200 rpm with 10 balls (using 0.15 g of $BaTiO_3$ powder for 30 mL $\sim$5 mg L^{-1} concentrated MB dye), there is negligible change in the morphology as well as in particle size, as before and after milling, the particle size was estimated as 0.5615 and 0.5225 μm, respectively. The absorbance spectrum shown in Fig. 5(a) supports the effect of particle size as there is no decrease in absorption spectrum with time; however, if there was a decrease in particle size, then surely the absorbance spectrum would increase. Thus, there was no effect on particle size with time in piezocatalysis through the ball milling technique in 60 min. Finally, the scavenger test was adopted to check the radicals responsible for the piezocatalysis process through ball milling. As discussed, during the piezocatalysis process, charges get separated, resulting in an induced surface potential. The

Open Access Article. Published on 23 ianuarie 2023. Downloaded on 07.01.2026 20:12:19.
This article is licensed under a Creative Commons Attribution-NonCommercial 3.0 Unported Licence.

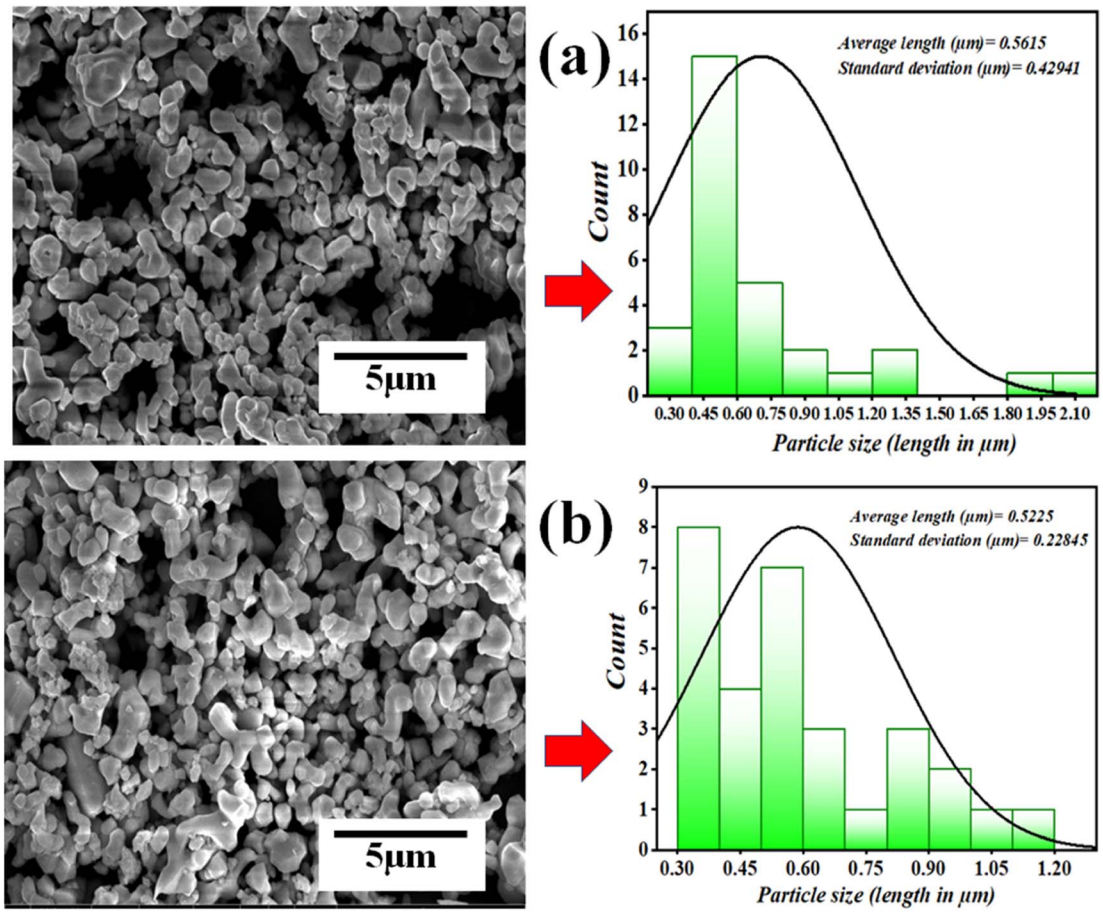

Fig. 11 SEM micrographs depicting particle size (a) before ball milling, (b) after ball milling.

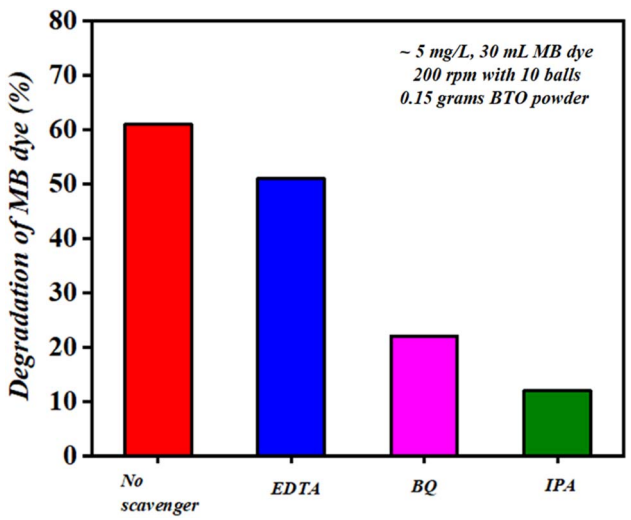

Fig. 12 Scavenger test for degradation of MB dye.

charges on the surface create reactive species from the water itself, such as holes (h^+), hydroxyl radicals ($^{\bullet}OH$), electrons (e^-), and superoxide radicals ($^{\bullet}O_2^-$), which are responsible for the demineralization of MB dye. However, every scavenger has the property of trapping a particular reactive species. In the present study, 100 μL of ethylenediaminetetraacetic acid (EDTA), isopropanol (IPA), and benzoquinone (BQ) were added to 30 mL of MB dye at 200 rpm with 10 milling balls using 0.15 g of $BaTiO_3$ powder. Ethylenediaminetetraacetic acid (EDTA), isopropanol (IPA), and benzoquinone (BQ) trap holes (h^+), hydroxyl radicals ($^{\bullet}OH$), and superoxide radicals ($^{\bullet}O_2$), respectively.[52,53]

Fig. 12 shows the degradation achieved by each scavenger under the ball milling technique. For EDTA, BQ, and IPA scavengers, the degradation was calculated as ~50, ~22, and ~12%, respectively, and the radicals present follow the order as (h^+) > ($^{\bullet}O_2^-$) > ($^{\bullet}OH$). The degradation achieved using IPA scavenger was found to be the least among all scavengers; thus, it can be stated that hydroxyl radicals ($^{\bullet}OH$) were the prime reactive species responsible for degrading 30 mL MB dye through piezocatalysis process by ball milling technique at 200 rpm with 10 balls using 0.15 g of piezocatalyst (BTO powder).

4. Conclusions

The present study brings out a new aspect of utilizing ball milling for the degradation of organic dyes. Ferroelectric $BaTiO_3$ powder having a tetragonal phase was used as a piezocatalyst for degrading ~5 mg L^{-1} of concentrated 30 mL and

© 2023 The Author(s). Published by the Royal Society of Chemistry

Open Access Article. Published on 23 ianuarie 2023. Downloaded on 07.01.2026 20:12:19.
This article is licensed under a Creative Commons Attribution-NonCommercial 3.0 Unported Licence.

50 mL MB dye. It was found that with an increase in the speed of ball milling and quantity of milling balls, the degradation of MB dye was increased. The high speed and quantities of milling balls generate a larger force, which as a result, produces more reactive species causing more degradation of MB dye as compared to other piezocatalysis systems. In the present study, maximum degradation was found to be ~77% with 15 balls at 300 rpm for 30 mL (~5 mg L^{-1} concentrated) MB dye using 0.30 g of $BaTiO_3$ powder in 60 min. Thus, the degradation of organic dyes *via* ball milling opens up novel possibilities in water remediation at a large scale.

Conflicts of interest

There are no conflicts to declare.

References

1 Y. C. Ho, K. Y. Show, X. X. Guo, I. Norli, F. M. A. Abbas and N. Morad, Industrial discharge and their effect to the environment, *Ind. Waste*, 2012, 1–33.
2 C. Fernández, M. S. Larrechi and M. P. Callao, An analytical overview of processes for removing organic dyes from wastewater effluents, *TrAC, Trends Anal. Chem.*, 2010, **29**(10), 1202–1211.
3 F. Bößl, T. P. Comyn, P. I. Cowin, F. R. García-García and I. Tudela, Piezocatalytic degradation of pollutants in water: Importance of catalyst size, poling and excitation mode, *Chem. Eng. J. Adv.*, 2021, **7**, 100133.
4 Y. Lin, S. Lai and J. M. Wu, Simultaneous piezoelectrocatalytic hydrogen-evolution and degradation of water pollutants by quartz microrods@ few-layered MoS2 hierarchical heterostructures, *Adv. Mater.*, 2020, **32**(34), 2002875.
5 J. Ling, K. Wang, Z. Wang, H. Huang and G. Zhang, Enhanced piezoelectric-induced catalysis of $SrTiO_3$ nanocrystal with well-defined facets under ultrasonic vibration, *Ultrason. Sonochem.*, 2020, **61**, 104819.
6 J. Dai, N. Shao, S. Zhang, Z. Zhao, Y. Long, S. Zhao, *et al.*, Enhanced piezocatalytic activity of Sr0. 5Ba0. $5Nb_2O_6$ nanostructures by engineering surface oxygen vacancies and self-generated heterojunctions, *ACS Appl. Mater. Interfaces*, 2021, **13**(6), 7259–7267.
7 P. Wang, X. Li, S. Fan, X. Chen, M. Qin, D. Long, *et al.*, Impact of oxygen vacancy occupancy on piezo-catalytic activity of BaTiO3 nanobelt, *Appl. Catal., B*, 2020, **279**, 119340.
8 A. Zhang, Z. Liu, B. Xie, J. Lu, K. Guo, S. Ke, *et al.*, Vibration catalysis of eco-friendly $Na_{0.5}K_{0.5}NbO_3$-based piezoelectric: An efficient phase boundary catalyst, *Appl. Catal., B*, 2020, **279**, 119353.
9 Y. Zhang, M. Xie, V. Adamaki, H. Khanbareh and C. R. Bowen, Control of electro-chemical processes using energy harvesting materials and devices, *Chem. Soc. Rev.*, 2017, **46**(24), 7757–7786.
10 F. Bößl and I. Tudela, Piezocatalysis: Can catalysts really dance?, *Curr. Opin. Green Sustainable Chem.*, 2021, **32**, 100537.
11 S. Kumar, M. Sharma, T. Frömling and R. Vaish, Antibacterial ferroelectric materials: Advancements and future directions, *J. Ind. Eng. Chem.*, 2021, **97**, 95–110.
12 D. Singh, A. Dixit and P. S. Dobal, Ferroelectricity and ferromagnetism in Fe-doped barium titanate ceramics, *Ferroelectrics*, 2021, **573**(1), 63–75.
13 W. Y. Shih, W.-H. Shih and I. A. Aksay, Size dependence of the ferroelectric transition of small $BaTiO_3$ particles: effect of depolarization, *Phys. Rev. B: Condens. Matter Mater. Phys.*, 1994, **50**(21), 15575.
14 G. H. Kwei, A. C. Lawson, S. J. L. Billinge and S. W. Cheong, *J. Phys. Chem.*, 1993, **97**, 2368–2377.
15 M. Sharma, R. Vaish and S. M. Ibrahim, Effect of poling condition on piezocatalysis activity of $BaTiO_3$-cement composites, *Mater. Lett.*, 2020, **280**, 128583.
16 D. Liu, C. Jin, F. Shan, J. He and F. Wang, Synthesizing $BaTiO_3$ nanostructures to explore morphological influence, kinetics, and mechanism of piezocatalytic dye degradation, *ACS Appl. Mater. Interfaces*, 2020, **12**(15), 17443–17451.
17 L. Chen, Y. Jia, J. Zhao, J. Ma, Z. Wu, G. Yuan, *et al.*, Strong piezocatalysis in barium titanate/carbon hybrid nanocomposites for dye wastewater decomposition, *J. Colloid Interface Sci.*, 2021, **586**, 758–765.
18 W. Qian, K. Zhao, D. Zhang, C. R. Bowen, Y. Wang and Y. Yang, Piezoelectric material-polymer composite porous foam for efficient dye degradation via the piezo-catalytic effect, *ACS Appl. Mater. Interfaces*, 2019, **11**(31), 27862–27869.
19 S. Lan, Y. Chen, L. Zeng, H. Ji, W. Liu and M. Zhu, Piezo-activation of peroxymonosulfate for benzothiazole removal in water, *J. Hazard. Mater.*, 2020, **393**, 122448.
20 Y.-L. Liu and J. M. Wu, Synergistically catalytic activities of $BiFeO_3/TiO_2$ core-shell nanocomposites for degradation of organic dye molecule through piezophototronic effect, *Nano Energy*, 2019, **56**, 74–81.
21 S. Lan, J. Feng, Y. Xiong, S. Tian, S. Liu and L. Kong, Performance and mechanism of piezo-catalytic degradation of 4-chlorophenol: finding of effective piezo-dechlorination, *Environ. Sci. Technol.*, 2017, **51**(11), 6560–6569.
22 H. You, X. Ma, Z. Wu, L. Fei, X. Chen, J. Yang, *et al.*, Piezoelectrically/pyroelectrically-driven vibration/cold-hot energy harvesting for mechano-/pyro-bi-catalytic dye decomposition of $NaNbO_3$ nanofibers, *Nano Energy*, 2018, **52**, 351–359.
23 J. Wu, N. Qin and D. Bao, Effective enhancement of piezocatalytic activity of $BaTiO_3$ nanowires under ultrasonic vibration, *Nano Energy*, 2018, **45**, 44–51.
24 M. Sharma, G. Singh and R. Vaish, Dye degradation and bacterial disinfection using multicatalytic $BaZr_{0.02}Ti_{0.98}O_3$ ceramics, *J. Am. Ceram. Soc.*, 2020, **103**(9), 4774–4784.
25 M. Sharma, V. P. Singh, S. Kumar and R. Vaish, Multicatalytic behavior of $Ba_{0.85}Ca_{0.15}Ti_{0.9}$ $Zr_{0.1}O_3$ ceramics for pharmaceutical/dye/bacterial treatments, *J. Appl. Phys.*, 2020, **127**(13), 135103.
26 M. Sharma, A. Halder and R. Vaish, Effect of Ce on piezo/photocatalytic effects of $Ba_{0.9}Ca_{0.1}Ce_xTi_{1-x}O_3$ ceramics for

Open Access Article. Published on 23 ianuarie 2023. Downloaded on 07.01.2026 20:12:19.
This article is licensed under a Creative Commons Attribution-NonCommercial 3.0 Unported Licence.

dye/pharmaceutical waste water treatment, *Mater. Res. Bull.*, 2020, **122**, 110647.
27 L. Qifeng, M. Jingjun, M. Sharma and R. Vaish, Photocatalytic, piezocatalytic, and piezo-photocatalytic effects in ferroelectric $(Ba_{0.875}Ca_{0.125})(Ti_{0.95}Sn_{0.05})O_3$ ceramics, *J. Am. Ceram. Soc.*, 2019, **102**(10), 5807–5817.
28 M. Sharma and R. Vaish, Piezo/pyro/photo-catalysis activities in $Ba_{0.85}Ca_{0.15}$ $(Ti_{0.9}Zr_{0.1})_{1-x}Fe_xO_3$ ceramics, *J. Am. Ceram. Soc.*, 2021, **104**(1), 45–56.
29 M. Sharma and R. Vaish, Vibration energy harvesting for degradation of dye and bacterial cells using cement-based $Ba_{0.85}Ca_{0.15}Zr_{0.1}Ti_{0.90}O_3$ composites, *Mater. Today Commun.*, 2020, **25**, 101592.
30 Y. Wang and K. Chang, Piezopotential-Induced Schottky Behavior of $Zn_{1-x}SnO_3$ Nanowire Arrays and Piezophotocatalytic Applications, *J. Am. Ceram. Soc.*, 2016, **99**(8), 2593–2600.
31 S. Komarov, T. Yamamoto, Y. Fang and D. Hariu, Combined effect of acoustic cavitation and pulsed discharge plasma on wastewater treatment efficiency in a circulating reactor: A case study of Rhodamine B, *Ultrason. Sonochem.*, 2020, **68**, 105236.
32 M. Awano, H. Takagi and Y. Kuwahara, Grinding effects on the synthesis and sintering of cordierite, *J. Am. Ceram. Soc.*, 1992, **75**(9), 2535–2540.
33 A. A. Kolchugin, E. Y. Pikalova, N. M. Bogdanovich, D. I. Bronin, S. M. Pikalov, S. V. Plaksin, *et al.*, Structural, electrical and electrochemical properties of calcium-doped lanthanum nickelate, *Solid State Ionics*, 2016, **288**, 48–53.
34 V. A. Sadykov, S. N. Pavlova, T. S. Kharlamova, V. S. Muzykantov, A. V. Ishchenko, A. S. Bobin, *et al.*, Perovskites and their nanocomposites with fluorite-like oxides as materials for solid oxide fuel cells cathodes and oxygen-conducting membranes: Mobility and reactivity of the surface/bulk oxygen as a key factor of their performance, in *Perovskites: Structure, Properties and Uses*, 2010, pp. 67–178.
35 C. Schumacher, J. G. Hernández and C. Bolm, Electro-mechanochemical atom transfer radical cyclizations using piezoelectric BaTiO3, *Angew. Chem., Int. Ed.*, 2020, **59**(38), 16357–16360.
36 Y. Pang, J. W. Lee, K. Kubota and H. Ito, Solid-State Radical C–H Trifluoromethylation Reactions Using Ball Milling and Piezoelectric Materials, *Angew. Chem., Int. Ed.*, 2020, **59**(50), 22570–22576.
37 K. Kubota, Y. Pang, A. Miura and H. Ito, Redox reactions of small organic molecules using ball milling and piezoelectric materials, *Science*, 2019, **366**(6472), 1500–1504.
38 F. Meng, W. Ma, Y. Wang, Z. Zhu, Z. Chen and G. Lu, A tribo-positive Fe@ MoS 2 piezocatalyst for the durable degradation of tetracycline: Degradation mechanism and toxicity assessment, *Environ. Sci.: Nano*, 2020, **7**(6), 1704–1718.
39 X. Liao, H. Xie, B. Liao, S. Hou, Y. Yu and X. Fan, Ball milling induced strong polarization electric fields in $Cu_3B_2O_6$ crystals for high efficiency piezocatalysis, *Nano Energy*, 2022, **94**, 106890.
40 Y. Shiratori, C. Pithan, J. Dornseiffer and R. Waser, Raman scattering studies on nanocrystalline $BaTiO_3$ Part I—isolated particles and aggregates, *J Raman Spectrosc*, 2007, **38**(10), 1288–1299.
41 A. Gajović, J. V. Pleština, K. Žagar, M. Plodinec, S. Šturm and M. Čeh, Temperature-dependent Raman spectroscopy of $BaTiO_3$ nanorods synthesized by using a template-assisted sol–gel procedure, *J. Raman Spectrosc.*, 2013, **44**(3), 412–420.
42 C. H. Perry and D. B. Hall, Temperature Dependence of the Raman Spectrum of $BaTiO_3$, *Phys. Rev. Lett.*, 1965, **15**(17), 700.
43 U. D. Venkateswaran, V. M. Naik and R. Naik, High-pressure Raman studies of polycrystalline $BaTiO_3$, *Phys. Rev. B: Condens. Matter Mater. Phys.*, 1998, **58**(21), 14256.
44 A. Gaur, M. Sharma, V. S. Chauhan and R. Vaish, Solar/visible light photocatalytic dye degradation using $BaTi_{1-x}Fe_xO_3$ ceramics, *J. Am. Ceram. Soc.*, 2022, **105**(8), 5140–5150.
45 L. Q. Wu, Y. C. Li, S. Q. Li, Z. Z. Li, G. D. Tang, W. H. Qi, *et al.*, Method for estimating ionicities of oxides using O 1s photoelectron spectra, *AIP Adv.*, 2015, **5**(9), 97210.
46 M. Rastogi, H. S. Kushwaha and R. Vaish, Highly efficient visible light mediated azo dye degradation through barium titanate decorated reduced graphene oxide sheets, *Electron. Mater. Lett.*, 2016, **12**(2), 281–289.
47 M. B. Starr and X. Wang, Fundamental analysis of piezocatalysis process on the surfaces of strained piezoelectric materials, *Sci. Rep.*, 2013, **3**(1), 1–8.
48 S.-Y. Lu, Q.-J. Mao, Z. Peng, X.-D. Li and J.-H. Yan, Simulation of ball motion and energy transfer in a planetary ball mill, *Chin. Phys. B*, 2012, **21**(7), 78201.
49 P. P. Chattopadhyay, I. Manna, S. Talapatra and S. K. Pabi, A mathematical analysis of milling mechanics in a planetary ball mill, *Mater. Chem. Phys.*, 2001, **68**(1–3), 85–94.
50 G. Singh, M. Sharma and R. Vaish, Transparent ferroelectric glass–ceramics for wastewater treatment by piezocatalysis, *Commun. Mater.*, 2020, **1**(1), 1–8.
51 R. Schmidt, H. Martin Scholze and A. Stolle, Temperature progression in a mixer ball mill, *Int. J. Ind. Chem.*, 2016, **7**(2), 181–186.
52 K. P. Singh, G. Singh and R. Vaish, Utilizing the localized surface piezoelectricity of centrosymmetric $Sr_{1-x}Fe_xTiO_3$ ($x \leq 0.2$) ceramics for piezocatalytic dye degradation, *J. Eur. Ceram. Soc.*, 2021, **41**(1), 326–334.
53 S. Mansingh, R. Acharya, S. Martha and K. M. Parida, Pyrochlore $Ce_2Zr_2O_7$ decorated over rGO: a photocatalyst that proves to be efficient towards the reduction of 4-nitrophenol and degradation of ciprofloxacin under visible light, *Phys. Chem. Chem. Phys.*, 2018, **20**(15), 9872–9885.

© 2023 The Author(s). Published by the Royal Society of Chemistry